

Investigation on Shell and Tube Heat Exchanger by Using CFD

A S Shukla¹, Mr. K. K. Bhabhor², Dr. D. B. Jani³

PG Student, M.E. CAD/CAM Department of Mechanical Engineering¹

Faculty, M.E. CAD/CAM Department of Mechanical Engineering^{2,3}

Government Engineering College, Dahod, Gujarat, India

Abstract: In this study, a detailed technique is built to examine the effectiveness of a shell and tube heat exchanger (STHE) with 35% baffle cuts (Bc) and variable numbers of baffles. Water was used as the working fluid in CFD simulations of a single pass and single tube heat exchanger. For this simulation investigation, a counterflow approach is used. The commercial CFD software package ANSYS-Fluent was utilized for computational analysis of STHE, and distribution of temperature was obtained due to the usage of copper and aluminum materials. In this research, the shell and tube heat exchanger was studied with the number of baffles of four, and six pieces by varying the mass flow rate value which is 0.5, 0.8, and 0.9. From this research, it was found that the highest total heat transfer rate and highest heat transfer coefficient is produced by copper with Six baffles at 0.9 mass flow rate.

Keywords: Shell and tube heat exchanger, Mass flow rate computational fluid dynamics (CFD), Ansys Fluent.

I. INTRODUCTION

Heat exchangers are devices that transmit thermal energy from a solid item to a fluid, or from two or more fluids to a solid object. A substantial wall might separate the fluids to prevent them from mixing, or they could be in direct contact. Space heating, refrigeration, air conditioning, power plants, petrochemical, chemical, and pharmaceutical industries, natural gas processing, and wastewater treatment are just a few of the applications.

In the STHE design, the baffling range and baffle gap are key characteristics. When baffle spaces are left larger or smaller than the optimum design, huge vortices of poorly dispersed flow, dead zones, and higher-pressure losses than expected occur. (Biçer et al., 2020)

According to research, 35–40% of heat exchangers used in industry are ST due to their strong structure and ease of maintenance. The use of baffles can help ST work more effectively. (Kunwer et al., 2020)

The shell-and-tube heat exchanger, as shown in Figure 1, is the most popular type of heat exchanger used in industrial applications. Heat exchangers with a large number of tubes are called shell-and-tube heat exchangers (sometimes several hundred) packed in a shell, axes parallel to the shell. Heat transfer takes place as one fluid flows inside the tubes while the other fluid flows outside the tubes through the shell. Baffles are typically used in the shell to push the shell-side fluid to flow across the shell, improving heat transfer and maintaining consistent tube spacing.

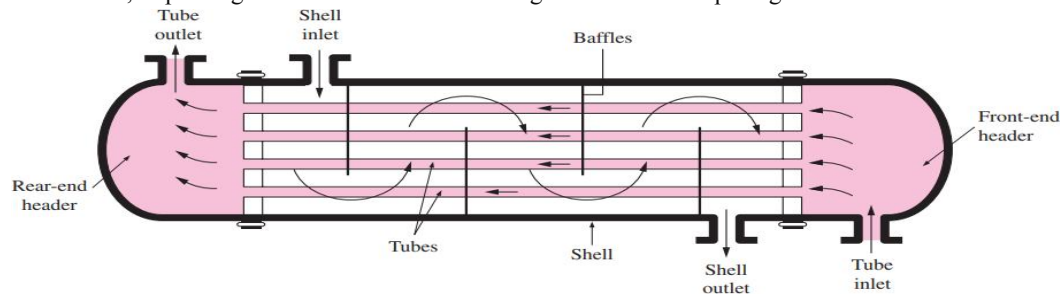


Figure 1 The schematic of a shell-and-tube heat exchanger (one-shell pass and one-tube pass)

A shell-and-tube heat exchanger's number of shell and tube passes is further classified. Heat exchangers with one-shell-pass and two-tube-pass heat exchangers, for example, have all of the tubes do one U-turn in the shell. A two-shell-passes and four-tube-passes heat exchanger, on the other hand, is known as a two-shell-passes and four-tube-passes heat exchanger. (Çengel, Yunus A, and Afshin J. Ghajar. Heat and Mass Transfer: Fundamentals & Applications. New York: McGraw-Hill)

Figure 2 (a) One-shell pass and two-tube passes

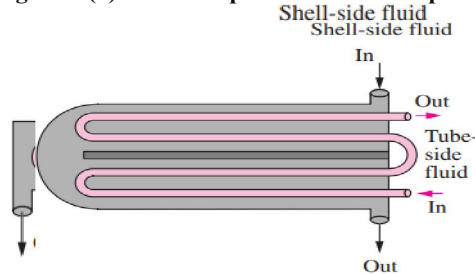


Figure 3 (b) Two-shell passes and four-tube passes

On the shell side of heat exchangers, baffles are used to support heat transfer tubes and govern shell-side flow distribution, which has a significant impact on heat transfer enhancement and thermal-hydraulic performance. (Wang et al., 2018)

Several quantitative design criteria, such as thermodynamic and geometric characteristics, are employed to arrive at an optimal heat exchanger design. The duty and corrosive properties of the process fluids will have an impact on the material used to create the specific device. (Vetrivel et al., 2015)

The different leakage channels and bypass streams that exist inside the various flow zones make shell side design particularly difficult; the leakages and streams vary depending on the shell design and size. Computational Fluid Dynamics (CFD) is a well-known industry technique that can visualize flow and temperature fields on the shell side, as well as simplify fault assessment and direct the designer in the right direction. (Vetrivel et al., 2015)

The material used and the number of baffles used has a big impact on the change in coefficient and heat transfer rate from STHE. The temperature outside the shell is affected by changes in material and the number of baffles. The pressure drop is affected by changes in material and the number of baffles inside the shell. (Permatasari & Yusuf, 2018)

The working fluids enter at the heat exchanger's opposing ends (i.e., counter-flow), and baffles are used to create turbulence and cross-flow velocity components, which raise the shellside fluid's convection coefficient. The combined effects of cross and counter flow configurations occur in this heat exchanger system. The baffles also prevent the tube bundle from bending and the impacts of fluid-induced vibration on the shell side. Tube sheets, which are welded to the shell body, secure the tubes. (Abeykoon, 2020)

Design of Shell and tube heat exchanger in Ansys Spaceclaim

For designing of model Ansys software 2020 R1 is used here are some key points for Ansys software:

- Ansys develops and markets engineering simulation software for use across the product life cycle
- Ansys Mechanical finite element analysis software is used to analyze the strength, toughness, elasticity, temperature distribution, electromagnetism, fluid flow, and other properties of structures, electronics, or machine components using computer models.
- Ansys is used to determine how a product will perform under various conditions without having to create test products or do crash tests.
- Ansys users often split down bigger structures into little components that are each designed and tested separately which is also known as Finite Element Analysis (FEA).

The shell and tube heat exchanger (STHE) geometry were adapted from the experimentally validated work of Ozden and Tari (2010) and some modifications is also done, which designed based on the standards of the Tubular Exchanger Manufacturers Association (TEMA).

Table 1 Geometric dimensions of shell and tube heat exchanger.

Variables	Dimensions
-----------	------------



Shell size D_s	90 mm
Tube outer diameter, d_o	19 mm
Tube bundle geometry and pitch	Triangular, 30 mm
Number of tubes, N_t	7
Heat exchanger length, L	600 mm
Shell side inlet temperature, T	300 K
Baffle cut B_c	35%
Number of baffles, N_b	6 and 4
Central baffle spacing, B	86 mm for 6 N_b and 120 mm for 4 N_b

Design of STHE in Ansys software

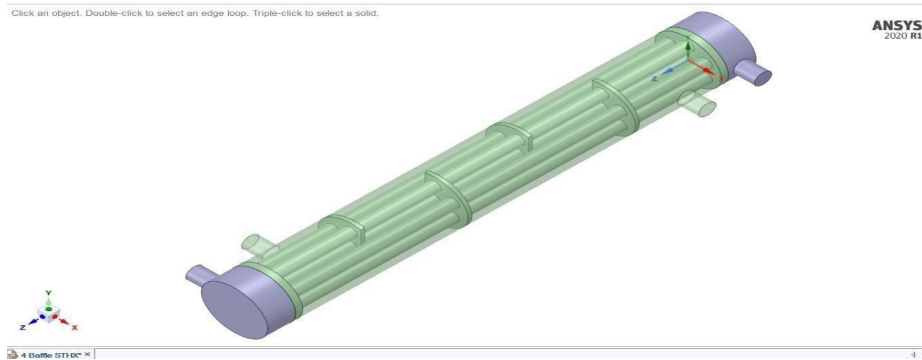


Figure 4 Isometric view of the arrangement of baffles and tubes of shell and tube heatexchanger with 4 baffles.

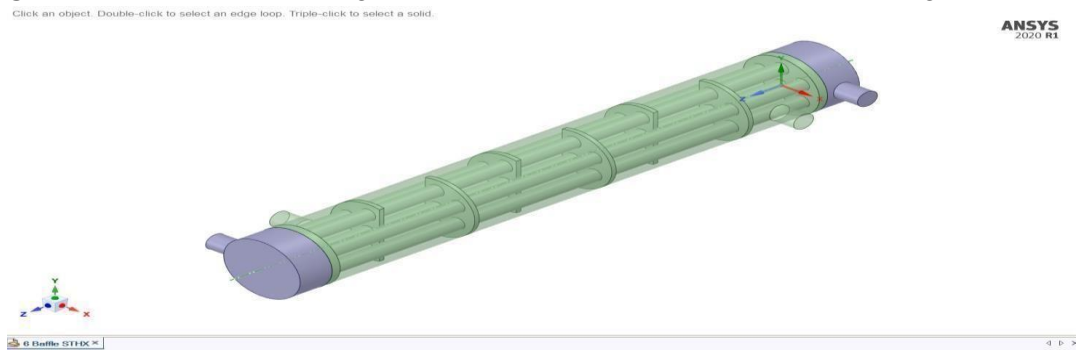


Figure 5 Isometric view of the arrangement of baffles and tubes of shell and tube heatexchanger with 6 baffles.

III. MESH SELECTION

ANSYS's default meshing client was used for meshing. The fine mesh with approximately 288784 elements will serve as data points for the temperature and flow of the fluids during the numerical simulation. Various combinations of automatic meshing methods developed in the program were used to disperse the mesh elements and nodes throughout the equipment. The mesh along the wall regions was controlled and concentrated using face and body selection.



Mesh generation is performed using Ansys software. The fine mesh with approximately 288784 elements. The STHE's resultant mesh is shown in Figure 3, and the mesh quality statistics are as follows: Number of Elements is 1063682 with fine mesh size and curvature angle $> 18^\circ$.

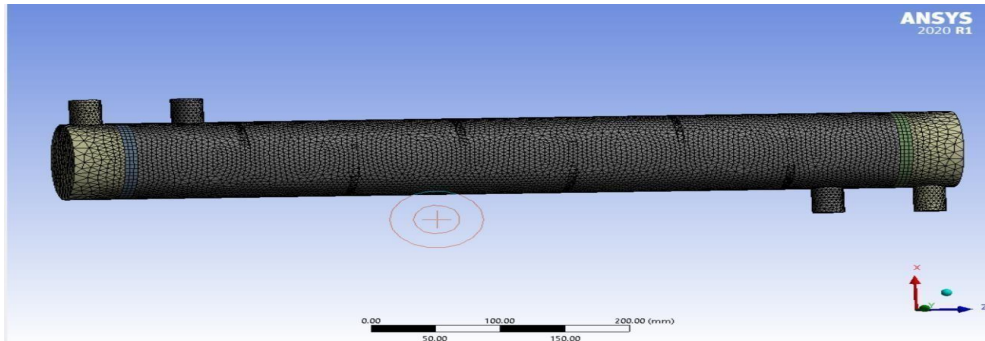


Figure 6 Meshing of Shell and Tube Heat Exchanger

IV. COMPUTATIONAL FLUID DYNAMICS (CFD)

CFD is the study of forecasting fluid flow, heat transfer, mass transfer, chemical reactions, and related phenomena by utilising a numerical algorithm (a computer) to solve the mathematical equations that govern these processes. CFD analyses produce important engineering data that can be used in conceptual design studies, detailed product development, troubleshooting, and redesign.

To use CFD, the geometry of interest is first divided into a number of computational cells, or discretized process of approximating differential equations by a system of algebraic equations for the variables at a set of discrete locations in space and time is known as discretization. The grid or mesh is the term for the discrete locations. ("Realize Greater Benefits from CFD," n.d.)

4.1 Advantage of CFD:

- Cost-cutting in development, obtaining necessary engineering data for design through physical experiments and tests can be costly.
- CFD simulations are quite affordable, and as computers become more powerful, costs are projected to reduce.
- Rapid evaluation of design variations, CFD simulations can be completed in a relatively short amount of time.
- Early in the design phase, engineering data might be introduced.
- Information that is comprehensive, Data can only be gathered from a restricted number of sites in the system during experiments (where sensors and gauges are placed).
- The designer can investigate any point in the region of interest using CFD and assess its performance using a set of thermal and flow metrics.
- CFD enables the theoretical simulation of any physical condition.
- CFD gives you a lot of control over the physical process and allows you to isolate individual phenomena for research.

4.2 Application of CFD

- Heat Transfer and Thermal Management Simulation in CFD
- Pipe and Valve Simulation with CFD
- Simulating Electronics Cooling with CFD
- Incompressible and Compressible Flow with CFD Simulation
- Turbo machinery CFD Simulation
- High Rheology Material CFD Simulation

V. RESULTS AND DISCUSSION



5.1 Problem Setup

ANSYS® FLUENT® 2020 R1 was used for simulation. For the simulation, the Fluent solver was used to select the Pressure Based type, absolute velocity formation, and steady time. The energy calculation option was enabled in the model, and the viscous was set to standard wall function (k-epsilon 2 equation).

Water-liquid fluid was chosen as the cell zone fluid. Water-liquid and copper aluminium were used as modelling materials. Inlet and outflow boundary conditions were chosen. Themass flow rate was set at 0.5, 0.8, and 0.9kg/s while temperature is set at 300k for cold inlet. At hot inlet also mass flow rate was set as 0.5,0.8 and 0.99kg/s and a temperature at 450K. In each input, the mass flow was chosen. In order to determine the relative pressure,drop between the inlet and output, the outlet nozzle is set to zero-gauge pressure. The velocity profile at the inlet is considered to be uniform. All surfaces have the no-slip condition. The shell exterior wall is given the zero-heat flux boundary condition, assuming the shell is completely insulated on the outside.

5.2 Convergence of Simulation

To obtain the parameters of the shell and tube heat exchanger in the exit, simulation convergence is necessary. It also provides exact parameter values for heat transfer rate requirements. The parts of scaled residual that must converge in a certain region are continuity, X-velocity, Y-velocity, Z-velocity, energy, k, and epsilon. X-velocity, Y- velocity, Z-velocity, k, epsilon should be less than 10-4 and energy should be less than 10-7for continuity.

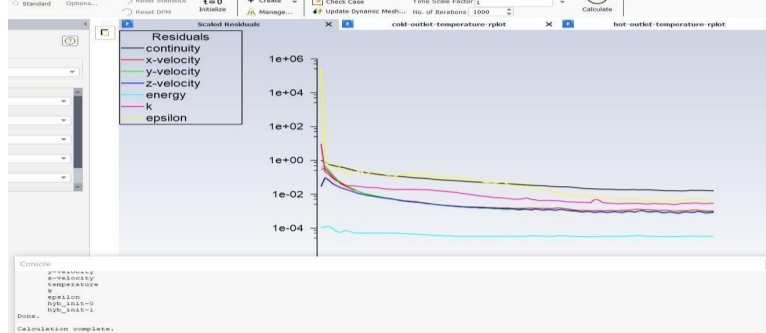


Figure 7 Convergence simulation

5.3 Variation of Temperature

Contour plots over the cross section at various baffle inclinations along the length of the heat exchanger will provide a detailed picture of the flow. In comparison to the number ofbaffle and mass flow rate 0.5,0.8, and 0.9, various temperature profile graphs are made.

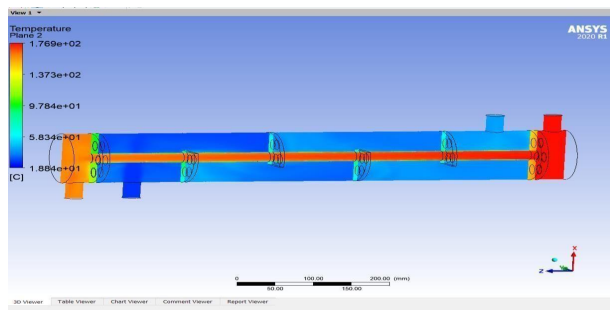


Figure 8 Temperature Distribution of 4 baffle at 0.5 kg/s.

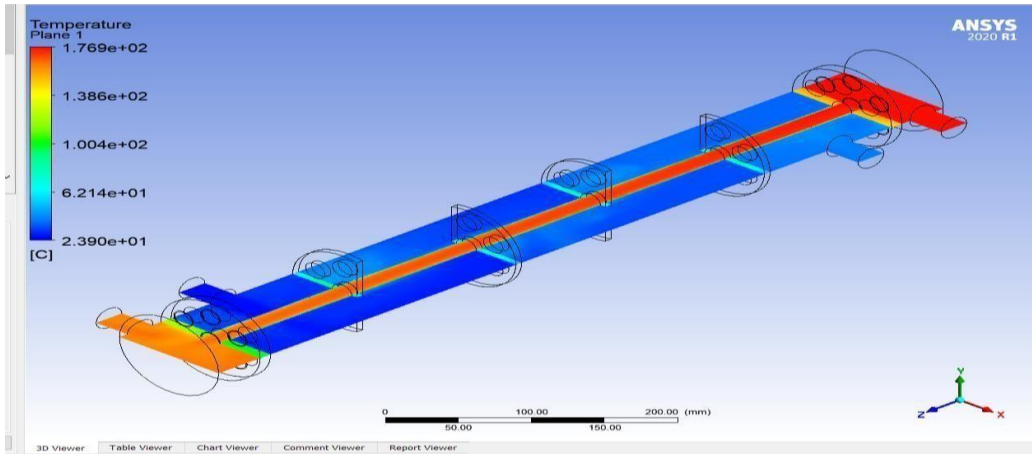


Figure 9 Temperature Distribution of 4 baffle at 0.8kg/s

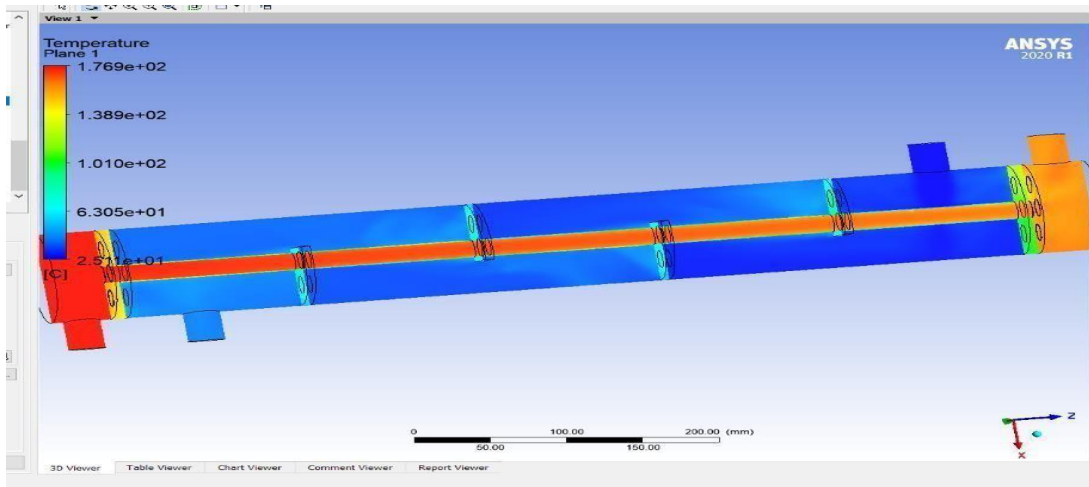


Figure 10 Temperature Distribution of 4 baffle at 0.9 kg/s.

Figures 4.9, 4.10 and 4.11 show the overall temperature profile of the cross-sections shown in the thermal contours, it is evident that the fluid near the inner tube is more heated than the fluid near the outer tubes. Thus, most of the heat transfer occurs due to the fluid near the inner tube, as depicted by the high temperature gradient near the center of the figures, versus the lower temperature gradient of the fluid far from the center of the shell. In the figures, it can be seen that regardless of the fluid used, heating is uniform until approximately 0.30 m of the heat exchanger, wherein a temperature gradient begins to appear.

5.4 Variation of Pressure

The below figure shows the pressure distribution across the shell and tube heat exchanger. The pressure drops inside the shell increase as the mass flow rate increases. By increasing the number of baffle pressure drop is also increase the pressure varies significantly from intake to output. The contours of static pressure are depicted in all of the figures to provide a more detailed understanding

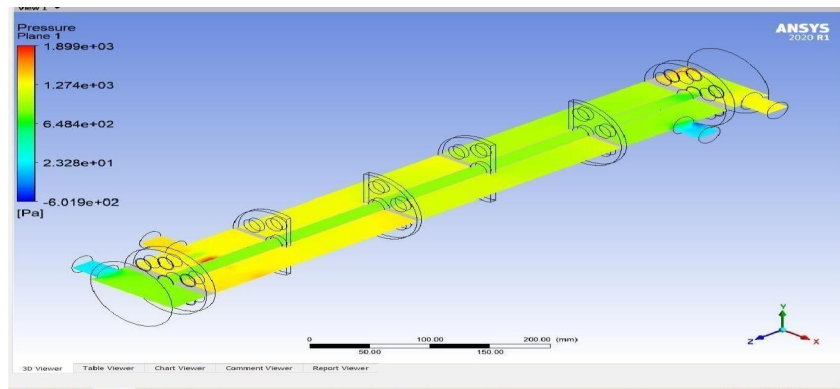


Figure 11 Pressure Distribution of 4 baffle at 0.5 kg/s

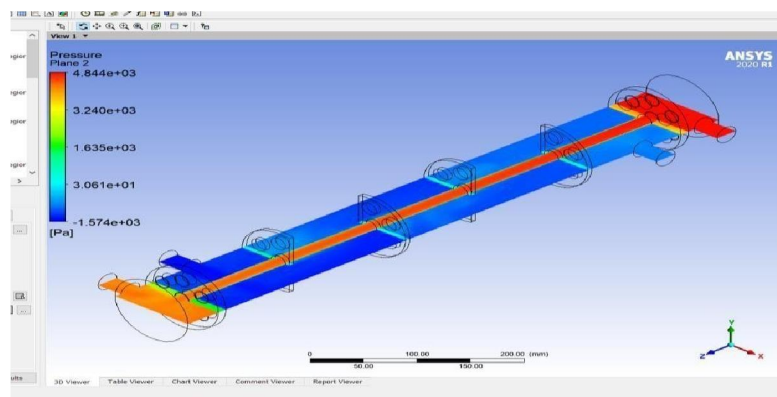


Figure 12 Pressure Distribution of 4 baffle at 0.8 kg/s.

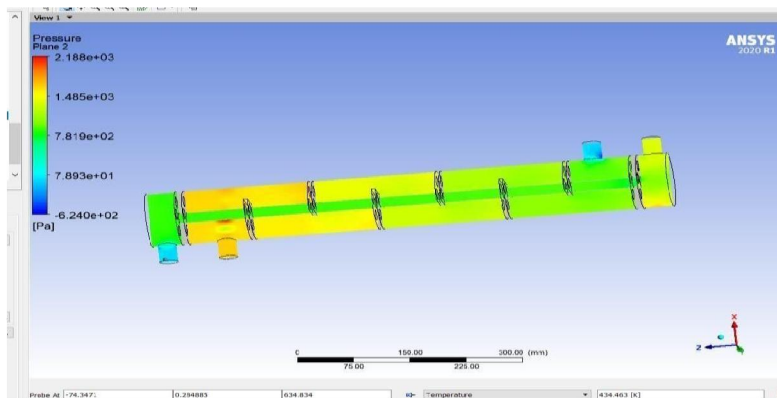


Figure 13 Pressure Distribution of 6 baffle at 0.5 kg/s

From the figure 4.11, 4.12 and 4.13 it was observed the highest-pressure drop were found with the 0.9kg/s mass flow rate having 4 and 6 baffles. By using the copper material value of pressure increase compare to aluminum material

5.4 Streamline the flow of hot and cold fluid:

In order to better understand the impact of nozzle and tube configuration on fluid pressure drop, streamlines are created for tube and shell. The color shows a decrease in speed due to the placement of a baffle inside the shell, the fluid's speed has decreased. It is observed that the flow hits the baffle plate, and the direction of the flow is changed. Therefore, the shell space behind the baffle is not effectively used for cross flow, as shown in Fig. 4.17 By using 4 and 6 baffles it is clear that as the number of baffles increases this region will be reduced and flow will be well developed.

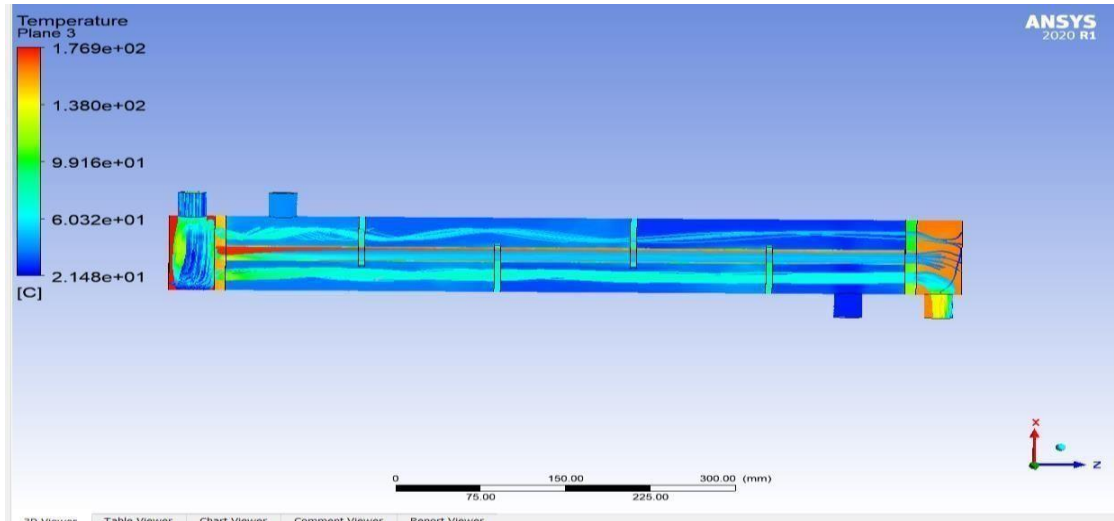


Figure 14 Streamline flow for tube fluid

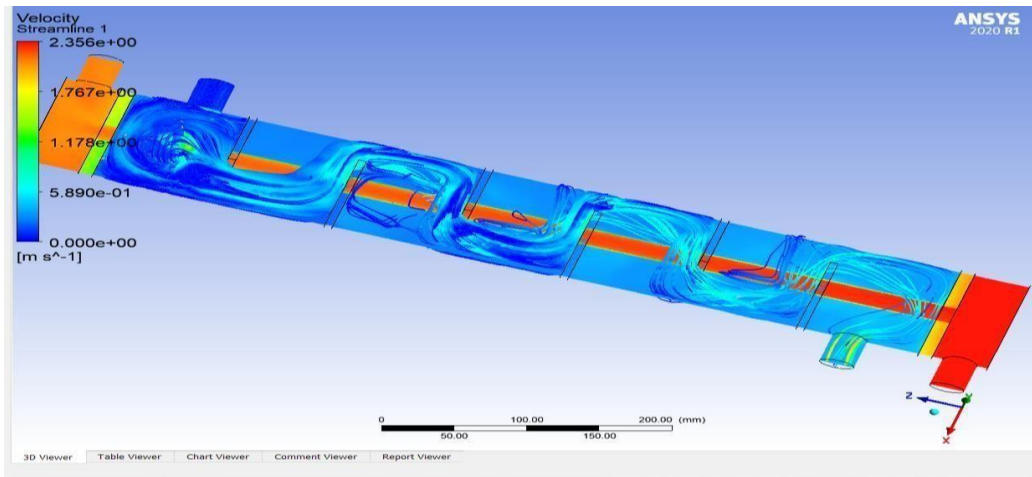


Figure 15 Streamline flow for Shell fluid.

4.6 Post Processing

The simulations' desired outcome is regulated in the post-processing stage. After calculating the solutions, ANSYS generates automatic reports for the fluxes and surface area variables. The parameters that are directly obtained from the ANSYS Fluent results are the total heat transfer rate, shell output temperature, and pressure drop. An equation was used to calculate the heat transfer coefficient, has follows:

$$h = Q/A (T_{wall} - T_{bulk}) \dots (1)$$

Here, Q is the total heat transfer rate, A is the heat transfer area

T_{wall} is the average wall temperature,

T_{bulk} is the bulk temperature and is the average of the inlet and outlet shell temperature

Total Heat Transfer Rate:

For validation of the total heat transfer rate given value was used

$$Q = m * C_p * \Delta T \dots (2)$$

Where m = mass flow rate

C_p = Specific Heat of Water

ΔT = Temperature Difference Between Shell Side



Nb	Mass flow rate(Kg/ s)	Result of CFD analysis		Analytical calculation
		Shell side outlet temp. (k)	Total heat transfer rate(w)	Total heat transferrate (w)
4	0.5	315.69	32808.49	32807.79
	0.8	314.209	47544.67	47537.79
	0.9	313.94	52486.33	52467.37
6	0.5	316.06	33607.68	33581.46
	0.8	314.617	49143.78	48902.63
	0.9	314.44	54412.26	54349.27

Table 2 Comparison between CFD and an analytical result of total heat transfer of aluminum:

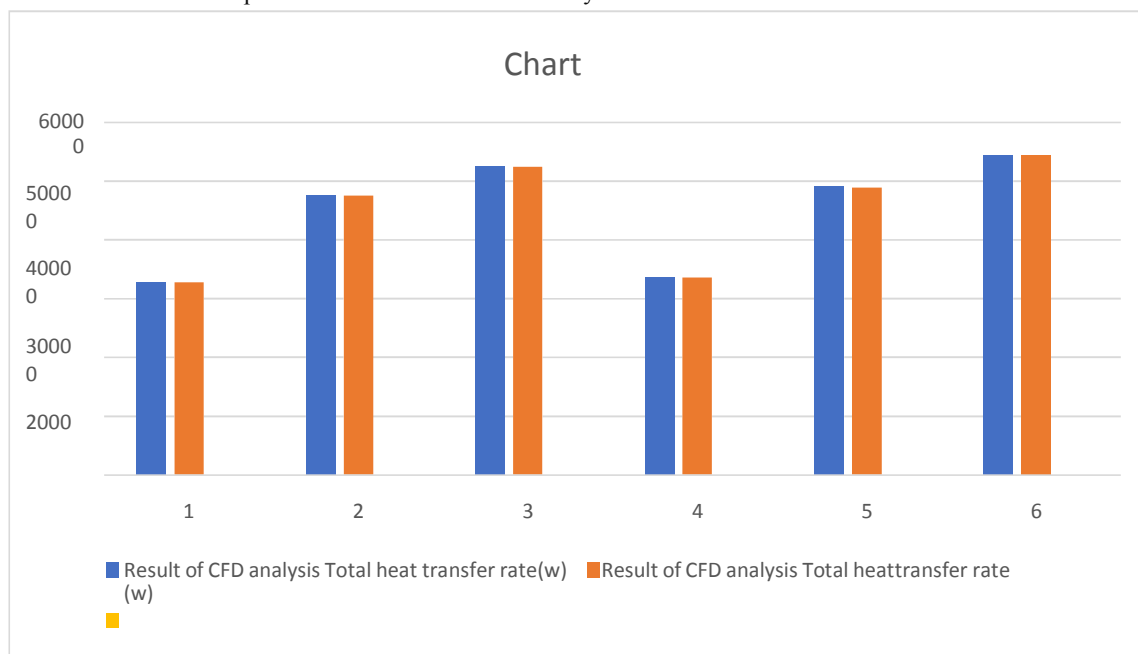


Figure 16 Bar chart of CFD and Analytical result of Total heat transfer rate (w)

CFD results are presented on the left side of the table. The shell side outlet temperature and shell side total heat transfer rate values are obtained directly from the Ansys fluent. The total heat transfer values are calculated using Equation 2 for validation. We can see from Tables 4-3 and in the bar chart, that the CFD value and theoretical very minor differences are present.

Table 3 Comparison between CFD and an analytical result of total heat transfer of copper.

Nb	Mass flow rate (Kg/ s)	Result of CFD analysis		Analytical calculation
		Shell side outlet temp. (k)	Total heat transferrate(w)	Total heat transferrate (w)
4	0.5	316.07	33576.13	33602.37
	0.8	314.6325	48961.4	48954.492
	0.9	314.3177	53902.8	53888.959
6	0.5	316.256	34029.54	33991.296
	0.8	314.8746	49798.09	497964.46
	0.9	314.6569	55226.91	55165.64



Figure 17 Bar chart of CFD and Analytical result of Total heat transfer rate (w).

It is observed from table 4.4 and bar chart 4.12 value of the Total heat transfer rate and shell sidetemperature of copper is more than the value of aluminum and the analytical method shows better agreement with the CFD result.

Table 4 Comparison of pressure drop of copper and aluminum

Nb	Mass flow rate (Kg/ s)	Pressure drops of aluminum	Pressure drops of copper
4	0.5	2500.58	2526.42
	0.8	6417.91	6410.06
	0.9	8144.03	8118.30
6	0.5	2811.72	2810.81
	0.8	7199.00	7190.30
	0.9	9083.00	9079.57

As the mass flow rate increases the value of pressure drop is also increased, when comparing the value of aluminum and copper, the pressure drop reduces comparatively in copper as the mass flow rate increase

Table 5 Comparison between CFD and an analytical result heat transfer coefficient

Nb	Mass flowrate (Kg/ s)	Result of CFD analysis		Analytical calculation	
		Shellside outlet temp. (k)	Heat transfer coeff. (W/m ² K)	Kern method Heat transfer coeff. (W/m ² K)	Bell-Delaware method Heat transfer coeff.(W/m ² K)
4	0.5	315.69	1440.00	1477.00	1560.4
	0.8	314.209	2190.99	1912.60	2134.8
	0.9	313.94	2408.73	2081.58	2273.8
6	0.5	316.06	1574.86	1796.00	1956.4
	0.8	314.617	2141.34	2367.70	2601.01
	0.9	314.44	2499.41	3185.76	2789.09

Table 5 summarizes the results of the present CFD model, as well as the differences between them and the data obtained using the Kern and Bell-Delaware method. In general, as the mass flow rate rises the shell outlet temperature decreases, and the heat transfer coefficient increases. It has been discovered that the Kern approach consistently underestimates the heat transfer coefficient. This is to be expected, as the Kern technique is a conservative approach. In the overall heat transfer coefficient calculation, the Bell– Delaware approach agrees better with the CFD results. In general, increasing the mass flow rate increases the difference. CFD results are compared to Bell–Delaware results for each parameter combination while selecting modeling parameters. Following the elimination of scenarios with unexpected outcomes, the case with the best agreement with the Bell– Delaware is chosen for modeling.

CFD results are presented on the left side of the table. The shell side outlet temperature, and total heat transfer rate values are obtained directly from the CFD runs. The heat transfer coefficient values are calculated using Equation 1. For the shell outlet value, the CFD values are utilized

VI. CONCLUSION

A small shell-and-tube heat exchanger's modelled in enough depth to resolve the flow and temperature fields. Shell side heat transfer coefficient, pressure drop, and heat transfer rate data are calculated using CFD simulation results for fixed tube wall and shell inlet temperatures. The mesh density, sequence of discretization, and turbulence modelling affect the sensitivity of the shell side flow and temperature distributions. For the Second- order discretization, the k–e realizable turbulence model with Second-order discretization and a fine mesh is chosen as the optimum simulation approach after comparison with Bell– Delaware results.

The simulation findings are compared to the results from the Kern and Bell–Delaware techniques by altering the number of baffles 4 and 6 and the baffle cut values of 35 percent 0.5, 0.8, and 0.9 kg/s mass flow rates. The Kern approach is found to consistently underestimate the heat transfer coefficient. The CFD simulation findings for suitably spaced baffles are found to be in extremely good agreement with the Bell–Delaware results. This research has led to the conclusion that changing the number of baffles, material selection, and mass flow rate plays a vital role in temperature outlet value, as well as other factors like total heat transfer rate and heat transfer coefficient.

REFERENCES

- [1]. Abbasian Arani, A. A., & Moradi, R. (2019). Shell and tube heat exchanger optimization using new baffle and tube configuration. *Applied Thermal Engineering*, 157. <https://doi.org/10.1016/j.applthermaleng.2019.113736>
- [2]. Abd, A. A., Kareem, M. Q., & Naji, S. Z. (2018). Performance analysis of shell and tube heat exchanger: Parametric study. *Case Studies in Thermal Engineering*, 12, 563–568. <https://doi.org/10.1016/j.csite.2018.07.009>
- [3]. Abeykoon, C. (2020). Compact heat exchangers – Design and optimization with CFD. *International Journal of Heat and Mass Transfer*, 146. <https://doi.org/10.1016/j.ijheatmasstransfer.2019.118766>
- [4]. Biçer, N., Engin, T., Yaşar, H., Büyükkaya, E., & Aydın, A. (2020). Design optimization of a shell-and-tube heat exchanger with novel three-zonal baffle by using CFD and Taguchi method. *International Journal of Thermal Sciences*, 155. <https://doi.org/10.1016/j.ijthermalsci.2020.106417>
- [5]. Bichkar, P., Dandgaval, O., Dalvi, P., Godase, R., & Dey, T. (2018). Study of Shell and Tube Heat Exchanger with the Effect of Types of Baffles. *Procedia Manufacturing*, 20, 195– 200. <https://doi.org/10.1016/j.promfg.2018.02.028>
- [6]. Cao, X., Zhang, R., Chen, D., Chen, L., Du, T., & Yu, H. (2021). Performance investigation and multi-objective optimization of helical baffle heat exchangers based on thermodynamic and economic analyses. *International Journal of Heat and Mass Transfer*, 176. <https://doi.org/10.1016/j.ijheatmasstransfer.2021.121489>
- [7]. Cruz, P. A. D., Yamat, E.-J. E., Nuqui, J. P. E., & Soriano, A. N. (2022). Computational Fluid Dynamics (CFD) analysis of the heat transfer and fluid flow of copper (II) oxide-water nanofluid in a shell and tube heat exchanger. *Digital Chemical Engineering*, 3, 100014. <https://doi.org/10.1016/j.dche.2022.100014>
- [8]. Effects of baffles and tube materials in the shell and tube heat exchanger using Computational fluid dynamics. (n.d.). <https://www.researchgate.net/publication/342065705>



- [9]. Elmekawy, A. M. N., Ibrahim, A. A., Shahin, A. M., Al-Ali, S., & Hassan, G. E. (2021). Performance enhancement for tube bank staggered configuration heat exchanger – CFD Study. *Chemical Engineering and Processing - Process Intensification*, 164. <https://doi.org/10.1016/j.cep.2021.108392>
- [10]. *Heat and Mass Transfer: Fundamentals and Applications*, 5/e. (n.d.).
- [11]. Kunwer, R., Pandey, S., & Sureshchandra Bhurat, S. (2020). Comparison of selected shell and tube heat exchangers with segmental and helical baffles. *Thermal Science and Engineering Progress*, 20. <https://doi.org/10.1016/j.tsep.2020.100712>
- [12]. Mahendran, J. (2020). Experimental analysis of shell and tube heat exchanger using flower baffle plate configuration. *Materials Today: Proceedings*, 21, 419–424. <https://doi.org/10.1016/j.matpr.2019.06.380>
- [13]. Permatasari, R., & Yusuf, A. M. (2018). Material selection for shell and tube heat exchanger using computational fluid dynamics method. *AIP Conference Proceedings*, 1977. <https://doi.org/10.1063/1.5043017>
- [14]. Rana, S., Zunaid, M., & Kumar, R. (2021). CFD simulation for heat transfer enhancement in phase change materials. *Materials Today: Proceedings*, 46, 10915–10921. <https://doi.org/10.1016/j.matpr.2021.02.006>
- [15]. Realize greater benefits from CFD. (n.d.). https://www.researchgate.net/publication/279893768_Realize_greater_benefits_from_CFD
- [16]. Salhi, J. E., Zarrouk, T., & Salhi, N. (2021). Numerical study of the thermo-energy of a tubular heat exchanger with longitudinal baffles. *Materials Today: Proceedings*, 45, 7306–7313. <https://doi.org/10.1016/j.matpr.2020.12.1213>
- [17]. Thondiyil, D., & Kizhakke Kodakkattu, S. (2019). Optimization of a shell and tube heat exchanger with staggered baffles using Taguchi method. *Materials Today: Proceedings*, 46, 9983–9988. <https://doi.org/10.1016/j.matpr.2021.04.092>
- [18]. Wang, S., Xiao, J., Wang, J., Jian, G., Wen, J., & Zhang, Z. (2018). Application of response surface method and multi-objective genetic algorithm to configuration optimization of Shell-and-tube heat exchanger with fold helical baffles. *Applied Thermal Engineering*, 129, 512–520. <https://doi.org/10.1016/j.applthermale ng.2017.10.039>

BIOGRAPHICAL NOTES



A. S. Shukla was born in Surat in India. He was graduated from Mahavir Swami College Engineering and Technology, Surat in 2019 and student of M.E CAD/CAM of Govt. Engineering college, Dahod. His areas of interest are Design, Manufacturing, renewable energy area related topics.



Mr K.K. Bhabhor currently working as an assistant professor in the Department of Mechanical engineering at Government Engineering College, Dahod under the Gujarat Technological university. Published more than 20 research paper in good Journals. His area of interests are Thermal Engineering, Solar energy, and Energy saving.



Dr. D.B. Jani received Ph.D. in Thermal Science (Mechanical Engineering) from Indian Institute of Technology (IIT) Roorkee. Ph.D. Supervisor at Gujarat Technological University (GTU). Published more than 100 Research Articles in International Conferences and Journals. Presently, he is an Associate Professor at Gujarat Technological University, GTU, Ahmedabad (Education Department, State of Gujarat, India, Class-I, Gazetted Officer). His area of research is Desiccant cooling, ANN, TRNSYS, Exergy